

# Efficient Probabilistic Assessment of Power System Resilience Using the Polynomial Chaos Expansion Method with Enhanced Stability

Aidan Gerkis\* and Xiaozhe Wang<sup>†</sup>

Department of Electrical and Computer Engineering  
McGill University

Montréal, Québec, Canada

Email: \*aidan.gerkis@mail.mcgill.ca, <sup>†</sup>xiaozhe.wang2@mcgill.ca

**Abstract**—Increasing frequency and intensity of extreme weather events motivates the assessment of power system resilience. The random nature of these events and the resulting failures mandates probabilistic resilience assessment, but state-of-the-art methods (e.g., Monte Carlo simulation) are computationally inefficient. This paper leverages the polynomial chaos expansion (PCE) method to efficiently quantify uncertainty in power system resilience. To address repeatability issues arising from PCE computation with different sample sets, we propose the integration of the Maximin-LHS experiment design method with the PCE method. Numerical studies on the IEEE 39-bus system illustrate the improved repeatability and convergence of the proposed method. The enhanced PCE method is then used to assess the resilience of the system and propose adaptation measures to improve it.

**Index Terms**—cascading failures, polynomial chaos expansion (PCE), power system resilience, uncertainty quantification

## I. INTRODUCTION

Climate change has resulted in increasing frequency and intensity of extreme weather events, posing a severe risk to the safe and secure operation of power systems. The ability of a power system to maintain its operation during these extreme events is encapsulated by the concept of resilience, defined as “the ability to limit the extent, system impact, and duration of degradation in order to sustain critical services following an extraordinary event” [1]. Quantifying resilience is an important step in the planning of power system investments.

To accomplish this task, Pantelli et al. [2] proposed the  $\Phi\Lambda E\Pi$  metrics, quantifying resilience through the magnitude and rate of performance degradation and restoration during a resilience event, but only evaluated these metrics within a deterministic framework. However, since extreme events and the resulting power system failures are random in nature, resilience must be analyzed in a probabilistic one. To this end, Monte Carlo simulation (MCS) has been applied to quantify resilience (e.g. by [3]–[5]), but this method is computationally inefficient, requiring a large number of simulations to accurately compute the probabilistic behaviour of resilience. To

improve the efficiency of MCS, scenario-based methods have been applied (e.g. by [6], [7]). These methods determine a set of “typical” values for the random sources, approximating the system’s average resilience with fewer model evaluations. However, scenario-based methods neglect the global (i.e. over all possible values of the random sources) resilience of the system. To overcome the computational challenge, Dobson et al. proposed a data-based method to assess cascading failures [8]. While promising, this method is limited by the small amount of available data, restricting its ability to provide a global assessment of resilience.

To achieve computational efficiency while capturing the complete distribution of uncertainty, recent works have applied the polynomial chaos expansion (PCE) method to power system problems [9], [10]. While these methods have successfully modelled uncertainty in many power system problems, they have not yet been applied to assess power system resilience. Additionally, they have been shown to suffer from stability issues (i.e. the repeatability of the PCE approximation with different sample sets) [11], affecting their applicability to real-world problems.

To address these challenges, this paper extends the AC Cascading Failure Model (AC-CFM) [12] to a discretized model of an extreme weather event. This model computes the system’s response to failures at each time step and assesses resilience through the  $\Phi\Lambda E\Pi$  metrics. The PCE method is then applied to efficiently quantify the probabilistic characteristics (i.e., mean, variance) of the resilience metrics. In particular, an enhanced experiment design method is proposed to overcome the stability problem seen with the conventional PCE method, ensuring repeatable results across different sample sets.

## II. RESILIENCE EVENT MODELING

Power system failures during an extreme weather event typically begin with the failure of a few components. These initial failures can trigger a cascade of failures throughout the network, causing widespread outages [12]. Cascading failures occur when a change in the power flow (due to a previous contingency) causes a component (e.g., transmission

The work is supported by Natural Sciences and Engineering Research Council (NSERC) Discovery Grant (NSERC RGPIN-2022-03236), Canada Research Chair Program, and Rubin & So Faculty Scholar Award.

line) to exceed its rated operating conditions, resulting in its disconnection from the network by a protection relay.

The AC-CFM model, proposed in [12], models cascading failures in a power system, calculating the system's response to a small set of initial contingencies. Firstly, the initial contingencies are disconnected from the network and the system state is updated by solving the AC power-flow problem. If this method fails to converge the model relaxes the problem by converting all load buses to dispatchable loads and then applies the optimal power flow method to compute the resulting system state. Once convergence is achieved, the AC-CFM model checks if any components (e.g., buses, branches, or generators) exceed their operating thresholds. Any that do are disconnected from the network to model the action of protection mechanisms, resulting in a new set of contingencies. This process repeats using the new set of contingencies until the system reaches a steady-state where no further protection mechanisms are triggered. Fig. 1 summarizes the AC-CFM model, and the reader is referred to Noebels et al. [12] for a detailed discussion and validation of the model.

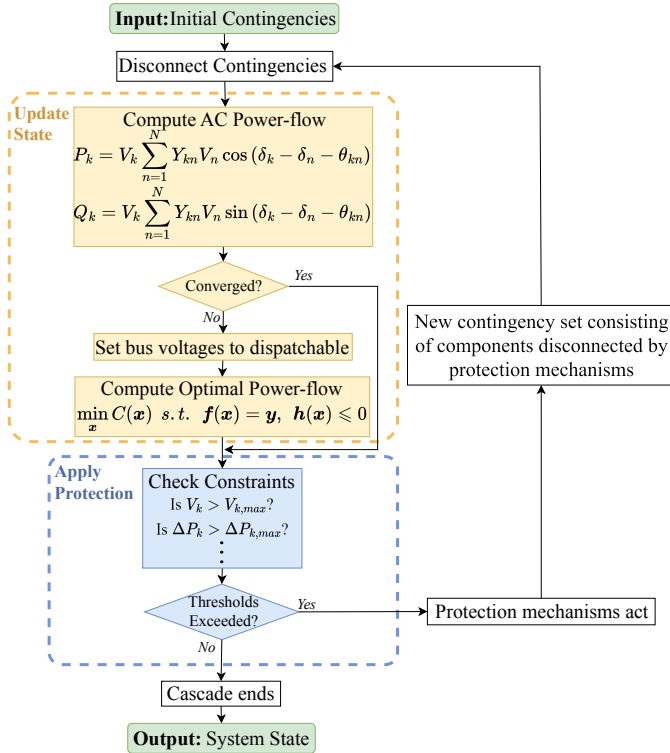


Fig. 1: The AC-CFM model proposed by Noebels et al. [12].

The AC-CFM model computes the response of a power system to a set of simultaneous contingencies, but extreme weather events typically consist of multiple non-simultaneous contingencies occurring over a long period. To address this, we extend the AC-CFM model to a discretized model of a weather event where contingencies occur at hourly intervals, chosen to reflect typical protection actions, which are completed within one hour of an initial failure [8]. The model input is a vector,  $\tau$ , whose components  $\tau_k$  represent the time at which the  $k$ -th component experiences a failure. At each time-step  $t_i$ , any components satisfying  $\tau_k = t_i$  are set as the initial

contingencies and the AC-CFM model calculates the resulting cascading failures and system state. This process is repeated at each time step to obtain the complete response to the extreme weather event.

To evaluate the resilience of the system we apply the  $\Phi\Lambda E\Pi$  metrics proposed by Pantelli et al. [2], which quantify the changes in a resilience indicator (i.e. a value quantifying the performance of the system) over time. We consider the load served indicator, whose value at time  $k$  is defined as

$$P_{\text{Served}}^{(k)} = \sum_{i \in \mathcal{L}} P_d^{(i,k)} \quad (1)$$

where  $\mathcal{L}$  is the set of load buses and  $P_d^{(i,k)}$  is the power demanded at load bus  $i$  at time  $k$ . To quantify resilience we apply the  $\Phi$  metric, which measures the rate at which the load served decreases during a resilience event and is computed as

$$\Phi_{LS} = \frac{P_{\text{Served}}^{(t_{\text{end}})} - P_{\text{Served}}^{(t_0)}}{t_{\text{end}} - t_0} \quad (2)$$

where  $t_0$  is the event start time and  $t_{\text{end}}$  is the event end time [2]. The resulting model may be expressed in the general form

$$\Phi_{LS} = \mathcal{M}(\tau) \quad (3)$$

where the input,  $\tau$ , is a vector representing the failure time of each component in the power system. The discretized weather model, its inputs  $\tau$ , and its output  $\Phi_{LS}$ , are summarized in Fig. 2.

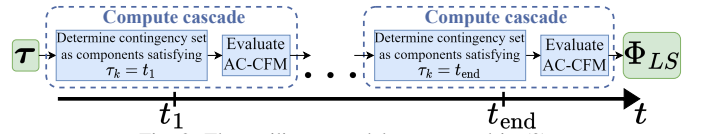


Fig. 2: The resilience model represented in (3).

The failure of a power system component during an extreme weather event is random, depending on the conditional probability of failure with respect to the weather state [2]. Therefore, the failure time for a given component,  $\tau_k$ , can be modelled by some probability distribution function (PDF)  $p_f^{(k)}$ . This PDF may be assumed to follow a known distribution (e.g. Gaussian or Weibull) or be computed from existing utility and weather data. In either case, the elements of the vector  $\tau$  can be drawn by randomly sampling these PDFs so that  $\tau_k \sim p_f^{(k)}$ . In large transmission networks, the extreme weather events may affect only part of the network, so the vector  $\tau$  may only represent a subset of all components.

While the mapping  $\mathcal{M}$  is deterministic in nature, the randomness in the input  $\tau$  will propagate to the output, making the  $\Phi_{LS}$  metric stochastic. Thus, to assess  $\Phi_{LS}$ , its statistical moments must be computed. The most common and straightforward method to accomplish this is MCS, which evaluates the moments by generating a large number of samples of  $\tau$  and evaluating (3) on each sample. However, this approach is computationally expensive, requiring a large number of evaluations of (3) to accurately compute the moments.

### III. POLYNOMIAL CHAOS EXPANSIONS

To overcome the inefficiency of the MCS method, PCE models of the  $\Phi_{LS}$  metric can be leveraged to efficiently evaluate its moments.

### A. Polynomial Chaos Expansion Theory & Computation

**PCE Theory:** The PCE method approximates the value of the  $\Phi_{LS}$  metric using a polynomial function of the form

$$\hat{\Phi}_{LS} = \sum_{i=1}^N c_i \Psi_i(\boldsymbol{\tau}) \quad (4)$$

where  $\Psi_i$  are multi-variate polynomials orthonormal with respect to the distribution of the random variable inputs, and  $c_i$  are deterministic coefficients [13]. If the function being modeled, (3), is continuous then it can be shown that (4) converges to  $\Phi_{LS}$  in the  $L^2$ -norm sense [13].

**The Experiment Design:** To compute the PCE representation in (4), a set of samples of the random inputs,  $\mathcal{X} = [\boldsymbol{\tau}^{(1)}, \dots, \boldsymbol{\tau}^{(N_S)}]^T$ , called the experiment, is required. The process of selecting the  $N_S$  samples is referred to as experiment design and is commonly accomplished via MCS or Latin-hypercube sampling (LHS) of the input vector. Experiment design via MCS is done by randomly sampling each component of the input vector according to its PDF, requiring many samples to accurately represent the input space. LHS improves the representation by dividing the input space into  $N_S$  equiprobable hypercubes and randomly placing one sample in each hypercube, providing more uniform coverage of the input space with fewer samples. In either case, (3) is then evaluated on each input sample, resulting in a vector of model outputs  $\Phi_{LS} = [\Phi_{LS}^{(1)}, \dots, \Phi_{LS}^{(N_S)}]^T$ , which is used to compute the PCE.

**Constructing the Polynomial Basis:** Before calculating the coefficients  $c_i$ , the multi-variate polynomial bases functions must first be defined. These polynomials,  $\Psi_{\alpha}(\boldsymbol{\tau})$ , are computed as the tensor product of univariate polynomials  $\psi_k^{(i)}(\tau_i)$  of degree  $k$  which are orthonormal with respect to the distribution of the  $i$ -th component of the random input vector  $\boldsymbol{\tau}$ ,

$$\Psi_{\alpha}(\boldsymbol{\tau}) = \prod_{i=1}^M \psi_{\alpha_i}^{(i)}(\tau_i) \quad (5)$$

where  $M$  is the dimension of  $\boldsymbol{\tau}$  and the multi-index notation is used to define the multi-variate polynomials. For some common distributions, known families of univariate orthonormal polynomials exist, but for others, the orthonormal polynomials can be computed through the Stieltjes procedure [13]. To improve sparsity in the PCE, the  $q$ -norm basis truncation scheme is adopted, limiting the the set of all bases  $\mathcal{A}$  to only multi-indices with a total degree  $p$  or less:

$$\mathcal{A}^q = \left\{ \boldsymbol{\alpha} \in \mathcal{A} : \left( \sum_{i=1}^M \alpha_i^q \right)^{1/q} \leq p \right\} \quad (6)$$

**Calculating the Coefficients:** For a given bases set  $\mathcal{A}^q$ , computation of the coefficient vector,  $\hat{\mathbf{c}}$ , is accomplished using the experiment,  $\mathcal{X}$ , and corresponding model evaluations,  $\Phi_{LS}$ , to compute the coefficient vector as

$$\hat{\mathbf{c}} = \min_{\mathbf{c}} \mathbb{E} [(\mathbf{c}^T \mathbf{A} - \Phi_{LS})^2] \quad (7)$$

where  $\mathbf{A}$  is the regression matrix, consisting of evaluations of the basis polynomials defined by  $\mathcal{A}^q$  on  $\mathcal{X}$ . Equation (7) is a least-squares regression problem, so a solution vector  $\hat{\mathbf{c}}$  may be obtained analytically. In practice, the Hybrid-LARS method

[13] is used to compute a sparse PCE by iteratively expanding the PCE basis, selecting the bases polynomials with the highest correlation to the residual and updating the coefficients until the desired accuracy is achieved.

### B. Post-Processing of the PCE

Once the PCE model is computed, the mean and variance of the  $\Phi_{LS}$  metric can be computed exactly from its coefficients.

$$\mu_{\Phi_{LS}} = \mathbb{E} [\hat{\Phi}_{LS}] = c_0 \quad (8)$$

$$\text{Var} [\Phi_{LS}] = \mathbb{E} \left[ \left( \hat{\Phi}_{LS} - \mu_{\Phi_{LS}} \right)^2 \right] = \sum_{\alpha \in \mathcal{A}^q \setminus 0} c_{\alpha}^2 \quad (9)$$

### C. The Challenges in Experiment Design and Estimation Consistency

The random sampling used to design the experiment,  $\mathcal{X}$ , means that PCEs built with two experiment designs will have different moment approximations. Consider Table I as an example. Two PCEs were built with different experiments of the same size. The PCE built with  $\mathcal{X}_1$  accurately approximates the moments, indicating convergence, while the other does not. The ability of a PCE to reliably converge when computed using different experiments of the same sample size is termed stability and is a critical barrier to the applicability of PCEs. If the PCE accuracy cannot be trusted to be consistent, how can the resulting PCE be usable?

TABLE I: Moment approximations obtained from two PCEs of the resilience model described in Section V built with different experiments with  $N_S = 30$ .

Method	$\mu$	Err( $\mu$ )	$\sigma$	Err( $\sigma$ )
MCS	-186.12	—	44.22	—
PCE - $\mathcal{X}_1$	-182.73	1.83%	43.47	1.69%
PCE - $\mathcal{X}_2$	-267.60	43.78%	641.63	1350.96%

## IV. A NOVEL EXPERIMENT DESIGN METHOD

To address the challenges in stability, a novel experiment design method, the Maximin-LHS method, is integrated into the PCE computation.

The conventional MCS method described in Section III-A may not sample the input space uniformly (see Fig. 3a). As a result, PCEs computed using an MCS experiment design require many samples,  $N_S$ , to obtain an acceptable estimation accuracy. The LHS method improves this by attempting to cover the input space more evenly with fewer samples, though it does not guarantee uniformity (see red dots in Fig. 3b).

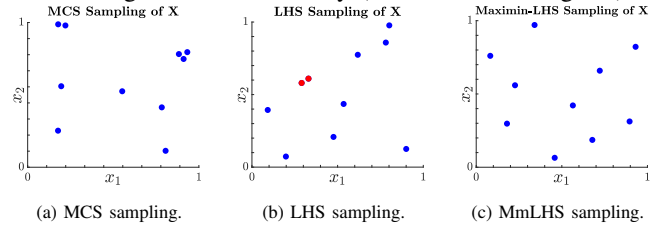


Fig. 3: Sampling of a 2-D random vector with both components uniformly distributed in  $[0, 1]$  using different methods.

To obtain a more uniform covering of the input space, the Maximin sampling method [14], which designs an experiment by placing  $N_S$  points so that the minimum distance between any two points is maximized, was introduced. Mathematically a Maximin experiment satisfies

$$\mathcal{X}_{Mm} = \max_{\mathcal{X}} \left\{ \min_{\mathbf{x}_1, \mathbf{x}_2 \in \mathcal{X}} \|\mathbf{x}_1 - \mathbf{x}_2\|_2 \right\} \quad (10)$$

One appeal of the Maximin experiment design is that it is D-optimal, implying that the information stored in the experiment is maximized [14].

While the Maximin method is theoretically sound, in practice it often results in experiments with sample points clumped on the boundaries of the input domain. To overcome this, Morris et al. proposed the Maximin-LHS (MmLHS) method [14] to design an experiment that satisfies (10) and forms a Latin hypercube. Such a design will share the uniform covering properties of the LHS designs while avoiding the issue of clumping and being D-optimal [14]. Although algorithms exist to compute MmLHS designs (e.g. the simulated annealing algorithm [14]), they are computationally complex and assume a uniform distribution of the random vector. Thus, we propose a new algorithm for finding approximate MmLHS designs:

- 1) Generate  $N_C$  candidate LHS designs,  $\mathcal{X}^{(i)}$ , of size  $N_S$ .
- 2) For each candidate design, compute the minimum Euclidean distance,  $d_{\min}^{(i)} = \min_{\mathbf{x}_1, \mathbf{x}_2 \in \mathcal{X}^{(i)}} \|\mathbf{x}_1 - \mathbf{x}_2\|_2$ .
- 3) Select the MmLHS experiment as  $\mathcal{X}_{MmLHS} = \mathcal{X}^{(k)}$  s.t.  $d_{\min}^{(k)} = \max_i \{d_{\min}^{(i)}\}$

Fig. 3c shows an MmLHS sampling obtained using this algorithm, clearly demonstrating an improved uniformity. This algorithm requires only the LHS design of  $N_C$  experiments, so the time to compute an MmLHS design is only slightly longer than that to compute an LHS design. For example, when designing experiments with  $N_S = 25$  and six random inputs  $t_{LHS} = 0.049s$  and  $t_{MmLHS} = 0.15s$ . Furthermore, since experiment design represents only a small fraction of the total PCE computation time (in the previous example  $t_{Total, LHS} = 911.41s$  and  $t_{Total, MmLHS} = 905.82s$ ), the additional time required for the MmLHS design is negligible. The PCE computation method leveraging the MmLHS sampling method is summarized in Fig. 4.

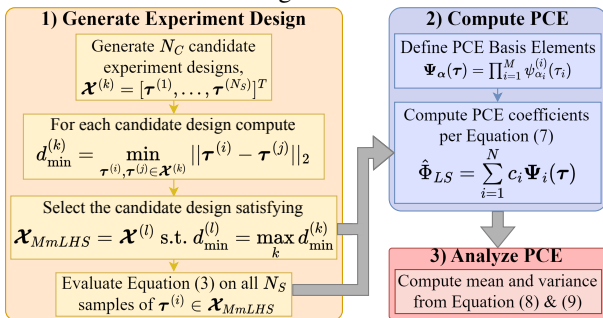


Fig. 4: The PCE uncertainty quantification method utilizing MmLHS experiment designs.

## V. CASE STUDY

### A. Simulation Setup

To evaluate the MmLHS experiment design method, PCEs were computed for the  $\Phi_{LS}$  metric in the IEEE 39-bus system subject to a windstorm. The windstorm was assumed to occur over a 24 hour period and affect a small area within the power system covered by buses 12, 13, 14, 15, 16, 17, & 20. It is assumed that component failures during the windstorm are primarily caused by wind damage to transmission lines and towers, so contingencies are modeled at the branches connecting the affected buses. Failure times for each branch follow the

probability distribution  $p_f(t)$ . To obtain this PDF, component failures during extreme windstorms in the Bonneville Power Administration [15] were correlated with discretized wind speed data [16] and the resulting failure probabilities were calculated for each discretized wind speed value. The response of the system to the resulting failures was computed using the model described in Fig. 2.

### B. Variance Calculation

While PCE models can accurately predict the behaviour of the  $\Phi_{LS}$  metric in the main body of the distribution they struggle with behaviour in the tails. As a result, the standard deviation approximation obtained from the PCE represents only the standard deviation of the main body of the distribution, not of the entire distribution [13]. In models with large outliers, which was the case in the simulated system, this can cause significant discrepancies between the true standard deviation and the PCE's estimate. To better assess PCE accuracy, it is more appropriate to compare the approximated standard deviation (hereafter referred to as "variance") with an outlier-robust measure from the validation data. For this purpose the median absolute deviation, computed for a dataset  $A$  as  $\sigma = \text{median}(A - \text{median}(A))$ , was used to compute the variance of the true model response.

### C. Stability Enhancement by the MmLHS Method

To assess and compare stability, experiments of different sizes  $N_S$  were generated using the MCS, LHS, and MmLHS methods, with 25 unique experiments being generated for each  $N_S$  and each method. Each point in Fig. 5a represents the average of the 25 mean approximations obtained from the PCE models computed with a specific sample size  $N_S$  and sampling method. The same procedure was repeated to obtain the remaining plots in Fig. 5 and 6. The moment approximations were validated by comparison to the mean and variance computed from 10,000 MCS of the model (the benchmark), represented by the dashed lines in Fig. 5a & 5b.

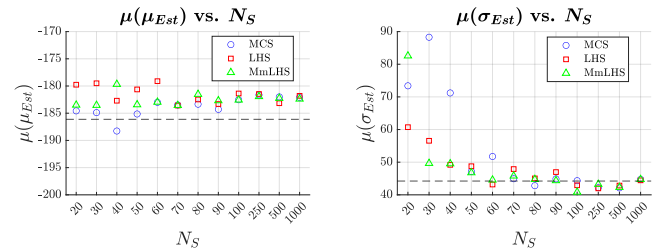


Fig. 5: The mean of the moment approximations versus  $N_S$ . The true moments are plotted in black.

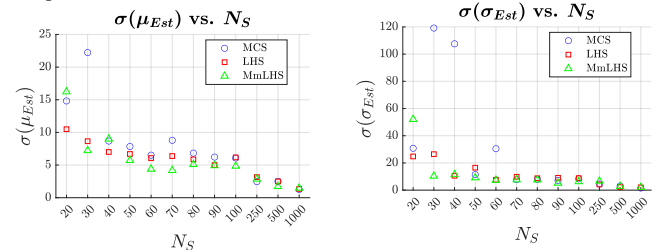


Fig. 6: The standard deviation of the moment approximations versus  $N_S$ .

Fig. 5a shows that the mean approximations are consistently accurate across all methods, with no significant improvements from the MmLHS method. However, it can be observed from Fig. 5b that the variance approximation converges with smaller  $N_S$  when using MmLHS, while MCS and LHS show decreases in accuracy at  $N_S = 60$  and  $N_S = \{70, 90\}$ , respectively. Fig. 6a demonstrates that the standard deviation of the mean approximations is consistently smaller with the MmLHS method for smaller  $N_S$  ( $N_S \in [50, 100]$ ). It is also observed from Fig. 6b that the standard deviation of the variance approximations decreases faster when using the MmLHS method, dropping to 10.32 when  $N_S = 30$ . After  $N_S = 30$ , the standard deviation for the MmLHS method remains low, indicating a stable approximation. In contrast, MCS and LHS show significant increases in variance standard deviation at  $N_S = 60$  and at  $N_S = 50$ , respectively.

These observations indicate that the MmLHS method obtains better stability in the PCE model and provides faster convergence for variance approximations, meaning that smaller experiment sizes can achieve accurate PCE models. For large  $N_S$ , all methods perform similarly, with the standard deviation of moment approximations, Fig. 6a and 6b, trending to 0. This is expected, as for large  $N_S$ , the PCE model is expected to converge regardless of the sampling method used [11].

#### D. Insights from the Resilience Assessment Results

To assess the power system’s resilience to the windstorm, we examine the the mean and variance approximations from the PCE model with the lowest computation error (Table II). The mean provides the system operator with an estimate of the expected rate of load-shedding in a typical failure scenario, which provides important guidance in the planning of adaptation measures (e.g., deployment of backup generation). However, the large variance indicates that actual load-shedding rates could significantly exceed the mean value. This observation highlights the importance of assessing the global behaviour of the  $\Phi_{LS}$  metric, as designing response measures based only on the mean value may result in inadequate preparedness. To address this, the variance may be used to generate confidence intervals for the  $\Phi_{LS}$  metric, enabling more robust decision-making. For example, the system operator may prepare by deploying backup generators or portable energy storage which can provide additional generation at a rate of  $-303.89$  MW/Hr (a lower bound on  $\Phi_{LS}$  computed by the  $3\sigma$  rule) to handle higher-than-expected load shedding and enhance the system’s resilience during the storm.

TABLE II: Approximated moments of the  $\Phi_{LS}$  metric, obtained from a PCE model computed with the Maximin-LHS method and  $N_S = 70$ .

Model	$\mu$ [MW/Hr]	Err( $\mu$ )	$\sigma$	Err( $\sigma$ )	$t_{\text{Total}}$
MCS	-186.12	—	44.22	—	208933.87s
PCE	-178.13	4.29%	41.92	5.20%	431.88s

## VI. CONCLUSION

In this paper, we proposed integrating the Maximin-LHS experiment design method with the PCE method for efficient probabilistic power system resilience assessment. Numerical

studies showed that the Maximin-LHS method can improve the stability of the PCE method and speed-up convergence, allowing smaller experiment sizes to achieve accurate PCE models. The PCE method can then be used to assess system resilience and direct response planning efforts. Future work includes the application of the Maximin-LHS method to different metamodeling techniques and the investigation of how the PCE method can be used to design adaptation measures for resilience enhancement.

## REFERENCES

- [1] A. M. Stanković, K. L. Tomsovic, F. De Caro, M. Braun, J. H. Chow, N. Cukalevski *et al.*, “Methods for analysis and quantification of power system resilience,” *IEEE Transactions on Power Systems*, vol. 38, no. 5, pp. 4774–4787, Sept. 2023.
- [2] M. Panteli, P. Mancarella, D. N. Trakas, E. Kyriakides, and N. D. Hatziaegyriou, “Metrics and quantification of operational and infrastructure resilience in power systems,” *IEEE Transactions on Power Systems*, vol. 32, no. 6, pp. 4732–4742, Nov. 2017.
- [3] X. Liu, K. Hou, H. Jia, Y. Mu, X. Yu, Y. Wang *et al.*, “A quantified resilience assessment approach for electrical power systems considering multiple transmission line outages,” in *2017 IEEE Electrical Power and Energy Conference (EPEC)*, 2017, pp. 1–5.
- [4] E. B. Watson and A. H. Etemadi, “Modeling electrical grid resilience under hurricane wind conditions with increased solar and wind power generation,” *IEEE Transactions on Power Systems*, vol. 35, no. 2, pp. 929–937, March 2020.
- [5] B. Li, D. Ofori-Boateng, Y. R. Gel, and J. Zhang, “A hybrid approach for transmission grid resilience assessment using reliability metrics and power system local network topology,” *Sustainable and Resilient Infrastructure*, vol. 6, no. 1-2, pp. 26–41, Jan. 2020.
- [6] W. Wang, L. Shi, and Z. Qiu, “Multi-indicator fused resilience assessment of power grids considering wind-photovoltaic output uncertainty during typhoon disasters,” *Electronics*, vol. 13, no. 4, Feb. 2024.
- [7] J. Zhou, H. Zhang, H. Cheng, S. Zhang, L. Liu, Z. Wang *et al.*, “Resilience-oriented hardening and expansion planning of transmission system under hurricane impact,” *CSEE Journal of Power and Energy Systems*, vol. 10, no. 4, pp. 1746–1760, Feb. 2024.
- [8] I. Dobson, “Estimating the propagation and extent of cascading line outages from utility data with a branching process,” *IEEE Transactions on Power Systems*, vol. 27, no. 4, pp. 2146–2155, Nov. 2012.
- [9] X. Wang, X. Wang, H. Sheng, and X. Lin, “A data-driven sparse polynomial chaos expansion method to assess probabilistic total transfer capability for power systems with renewables,” *IEEE Transactions on Power Systems*, vol. 36, no. 3, pp. 2573–2583, May 2021.
- [10] J. Liu, X. Wang, and X. Wang, “A sparse polynomial chaos expansion-based method for probabilistic transient stability assessment and enhancement,” in *2022 IEEE Power & Energy Society General Meeting (PESGM)*, Denver, CO, USA, 2022, pp. 1–5.
- [11] N. Fajraoui, S. Marelli, and B. Sudret, “Sequential design of experiment for sparse polynomial chaos expansions,” *SIAM/ASA Journal on Uncertainty Quantification*, vol. 5, no. 1, pp. 1061–1085, Jan. 2017.
- [12] M. Noebels, R. Preece, and M. Panteli, “Ac cascading failure model for resilience analysis in power networks,” *IEEE Systems Journal*, vol. 16, no. 1, pp. 374–385, March 2022.
- [13] G. Blatman, “Adaptive sparse polynomial chaos expansions for uncertainty propagation and sensitivity analysis,” Ph.D. dissertation, Université Blaise Pascal, Clermont-Ferrand, France, 2009, [Online]. Available: <https://sudret.ibk.ethz.ch/research/publications/doctoralTheses/g-blaman.html>.
- [14] M. D. Morris and T. J. Mitchell, “Exploratory designs for computational experiments,” *Journal of Statistical Planning and Inference*, vol. 43, no. 3, pp. 381–402, Feb. 1995.
- [15] Bonneville Power Administration, “Reliability & outage reports,” [Online]. Accessed: 2023-11-28, Available: <https://transmission.bpa.gov/BUSINESS/Operations/Outages/>.
- [16] Global Modeling and Assimilation Office (GMAO), “MERRA-2 inst1\_2d\_asm\_Nx: 2d,1-Hourly,Instantaneous,Single-Level,Assimilation,Single-Level Diagnostics V5.12.4,” 2015, greenbelt, MD, USA, Goddard Earth Sciences Data and Information Services Center (GES DISC). Accessed: 2023-12-18.